DNA-Binding Ability of GAGA Zinc Finger Depends on the Nature of Amino Acids Present in the β-Hairpin†

Muthu Dhanasekaran,[§,‡] Shigeru Negi,[§] Miki Imanishi,[#] and Yukio Sugiura*[,§]

Faculty of Pharmaceutical Sciences, Doshisha Women's University, Koudo, Kyotanabe-Shi 610-0395, Japan, and Institute for Chemical Research, Kyoto University, Uji 611 0011, Japan

Received January 2, 2007; Revised Manuscript Received April 22, 2007

ABSTRACT: The GAGA factor of *Drosophila melanogaster* uses a single Cys_2-His_2-type zinc finger for specific DNA binding. Comparative sequence alignment of the GAGA zinc finger core with other structurally characterized zinc fingers reveals that the β-hairpin of the GAGA zinc finger prefers amino acids with an aliphatic side-chain different from those of other zinc fingers. To probe the substitution effect of aromatic amino acids in the β-hairpin on the DNA binding, three mutant peptides were designed by substituting consensus phenylalanine, an aromatic amino acid, at key positions in the β-hairpin region. The metal-binding and the overall fold of the mutant peptides are very similar to those of the wild-type as shown by UV−vis absorption spectroscopy and circular dichroism spectroscopy. However, the gel mobility shift assay and isothermal calorimetric studies demonstrated that none of the mutants are able to bind the cognate DNA substrate, although the mutation is confined only to the β-hairpin region. The present results suggest that the nature of the amino acids in the β-hairpin plays an important role in the DNA-binding of the GAGA factor protein.

The DNA-binding ability of the zinc finger domain made it a potential molecule to be re-engineered into DNA-binding functional proteins (*1*−*3*). Many research groups used the classical Cys_2-His_2-type zinc finger framework to design artificial functional proteins with potential application in medicine (*4*−*6*). The GAGA factor of *Drosophila melanogaster* is particularly attractive because it uses a single Cys_2-His_2-type zinc finger for specific DNA binding (*7*). In general, the other naturally occurring zinc finger proteins require at least two zinc fingers linked in a tandem fashion for specific DNA recognition (*8*). Thus, the design of a DNA-binding functional protein with the GAGA zinc finger is not limited to the tandem assembly of multiple zinc fingers. Pedone et al. reported the minimal DNA-binding domain of GAGA (GAGA-DBD) by characterizing a series of deletion mutants (*7*). The minimal DNA-binding domain of the GAGA transcription factor (GAGA-DBD) is 63 residues in length and specifically binds to DNA derived from the h3/h4 promoter containing the sequence GAGAGAG with a dissociation constant of 5 nM. The specific DNA-binding ability of GAGA-DBD is lost when the N-terminal basic region is truncated. In 1997, the same research group shed light on the DNA-binding mode of the GAGA-DBD based on NMR studies of the peptide/DNA complex (*9*). They found that the structure as well as the DNA-binding mode is very similar to other classical Cys_2-His_2-type zinc fingers.

However, there is a striking difference in the amino acid preference in the β-hairpin region when compared to other structurally characterized zinc fingers. As clearly shown in Figure 1, the sequence alignment of the zinc fingers reveals that the amino acid preference in the short β-hairpin region of the zinc finger core of the GAGA protein is different from other proteins. In GAGA, the first position of β-strand 1 (β1) is occupied by the helix favoring alanine (*10*, *11*), and the third position of the β-strand 2 (β2) is occupied by isoleucine. On the contrary, almost all other known zinc fingers prefer aromatic amino acids at these positions. Among the aromatic amino acids, phenylalanine is highly conserved at the third position of β2, whereas phenylalanine, tyrosine, and histidine are preferred at the first position of β1. It is intriguing to note that nonaromatic amino acids are preferred in the β-hairpin region of the GAGA protein. The amino acids in the β2 were shown to be involved in the minimal hydrophobic core of the ββα architecture of the zinc finger (*12*). The role of a minimal hydrophobic core in the structural stability was proved by redesigning the artificial zinc finger peptides which assumed a ββα fold without metal but with a minimal hydrophobic core by juxtaposing hydrophobic amino acids (*13*, *14*). The substitution of a consensus phenylalanine residue with nonaromatic amino acid residues in the β-hairpin significantly decreased the thermodynamic or dynamic stability of the folded form of individual zinc fingers from other zinc finger proteins despite retaining the ββα structure (*15*−*17*). Therefore, it is of special interest to study the effect of the substitution of aromatic amino acids

† This study was supported in part by Grants-in-Aid for Scientific Research (14370755, 16659028, and 17390028) from the Ministry of Education, Culture, Sports, Science, and Technology, Japan, and Suntory Institute for Bioorganic Research, Japan. M.D. was supported by JSPS research fellowship from Japan Society for the Program of Science for foreign researchers.

* Corresponding author: Tel. +81-774-65-8649. Fax. +81-774-65-8652. E-mail: ysugiura@dwc.doshisha.ac.jp.

§ Doshisha Women's University.

Kyoto University.

‡ Present address: Department of Medicinal Chemistry, National Institute of Pharmaceutical Education and Research (NIPER), Sector 67, Phase X, Mohali, Punjab, 160-062, India.

10.1021/bi700009q CCC: $37.00
Published on Web 05/31/2007

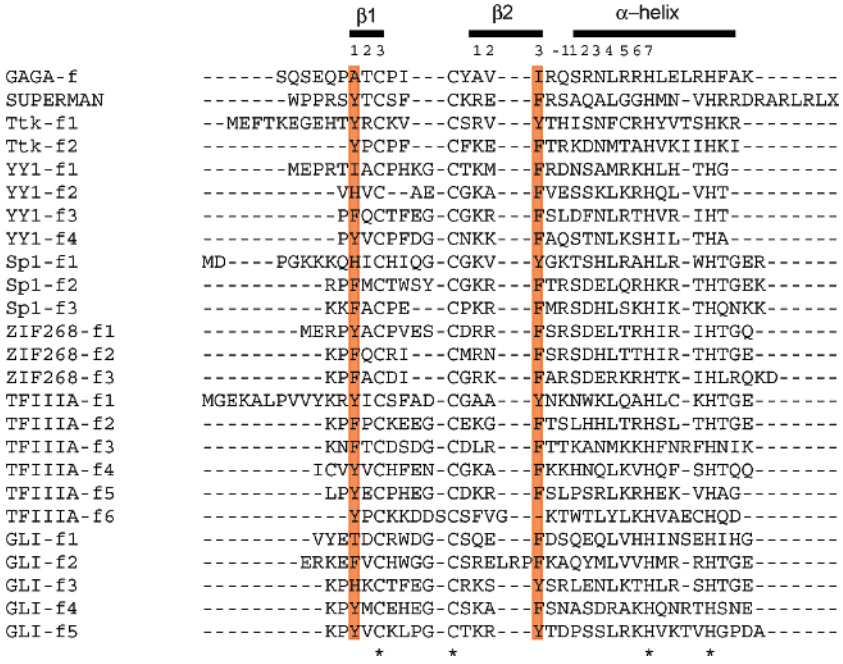

FIGURE 1: Sequence alignment of GAGA zinc finger core with other selected structurally characterized zinc fingers having the general structure (F/Y)−X−C−X(2−4)−C−X(3)−(F/Y)−X(5)−H−X(3−5)−H. Metal-binding residues (Cys and His) are indicated by an asterisk. The positions of the two β-strands and DNA-recognition helix are indicated by the position numbering within them. The key amino acid positions showing striking differences with the other zinc fingers are highlighted in red.

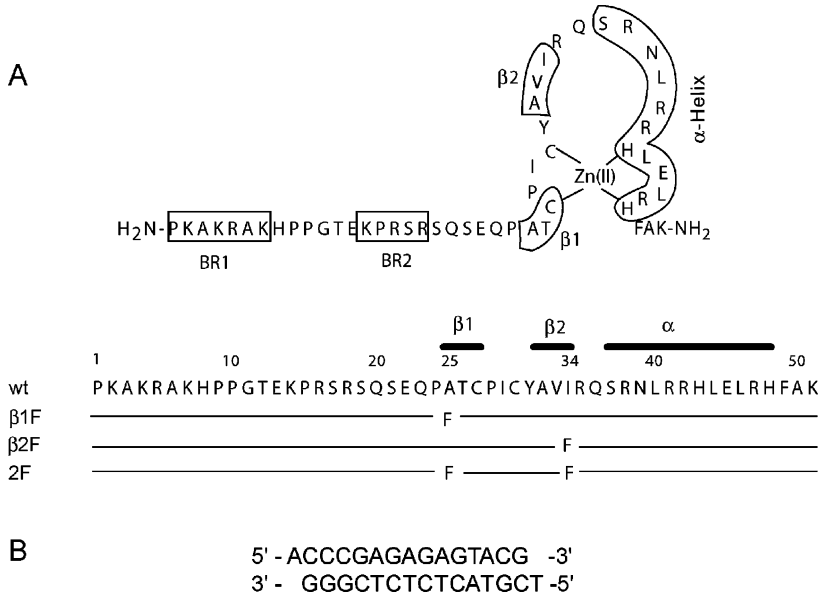

FIGURE 2: (A) Amino acid sequences of GAGA zinc finger mutant peptides and (B) DNA substrates used in this study.

at these positions on DNA binding, because the folding and DNA binding of the GAGA are very similar to the other structurally characterized zinc fingers. Furthermore, the role of the β-hairpin in the DNA binding was recently investigated by our group (*18*). The results strongly indicated that the β-hairpin region appears to function as a scaffold and has an important effect on the DNA-binding properties of the Cys_2-His_2-type zinc finger peptides. Moreover, in our continuous effort to design DNA-binding functional proteins, we would like to harness the potential of single zinc finger of the GAGA in our future design. In this paper, we report the folding and DNA-binding properties of peptide mutants having an aromatic amino acid substitution in the β-hairpin region of the minimal DNA-binding domain of the GAGA protein. The peptide sequences and the DNA substrate used in this study are shown in Figure 2. The wild-type GAGA-DBD (51 A.A.) used here was an N-terminal deletion sequence of the original GAGA-DBD (63 A.A.) reported by Pedone et al. (*7*). We have shown that this shorter peptide (51 A.A.) also specifically binds to the cognate DNA (*19*). The short peptide is advantageous because it can be reliably synthesized by a standard solid-phase peptide synthesis.

MATERIALS AND METHODS

Peptide Synthesis and Purification. The assembly of the peptide chain was performed on the Rink amide resin by the solid-phase method using a Shimadzu PSSM-8 synthesizer, with the Fmoc strategy with a slightly modified

protocol using HATU[1]/TMP as the coupling reagent (*20*). After the assembly, the peptides were cleaved from the resin using a cocktail consisting of 92.5% trifluoroacetic acid, 2.5% water, 2.5% ethanedithiol, and 2.5% triethylsilane for 90 min. The crude peptides were precipitated with ice-cold ether, separated by centrifugation, washed three times with diethyl ether, and finally dissolved in water and lyophilized. The peptide purification was performed using the RP-HPLC system, model L-7100 (Shimadzu Corp.) on a COSMOSIL RP-C_{18} column (10 × 250 mm) (Nacalai Tesque, Inc.) using a linear gradient with acetonitrile−water containing 0.1% trifluoroacetic acid. The purified peptides were characterized by RP-HPLC and laser desorption time-of-flight mass spectrometry (MALDI-TOF) using the Voyager-DE STR system (Applied Biosystems).

Ultraviolet−Visible Absorption Spectroscopy. The UV−vis absorption spectra were recorded on a Beckman Coulter DU7400 diode array spectrophotometer at 20 °C in Tris-HCl buffer (10 mM, pH 8.0) containing NaCl (50 mM) in a capped 1 cm path length cell. All presented spectra were normalized by $\epsilon = A/lc$, where ϵ is the extinction coefficient (M^{-1} cm^{-1}), l is the path length of the cell (cm), and c is the peptide concentration (M).

Circular Dichroism Spectroscopy. All the circular dichroism experiments were carried out using a JASCO J-720 spectropolarimeter. The spectra were recorded from 195 to 260 nm using the continuous mode with a 1 nm bandwidth, a 1 s response, and a scan speed of 50 nm min^{-1}. Each spectrum represents the average of 20 scans at 20 °C in Tris-HCl buffer (10 mM, pH 8.0) containing NaCl (50 mM) in a capped 0.1 cm path length cell under a nitrogen atmosphere. Thermal denaturation was monitored at 208 and 222 nm, acquiring data 10 °C intervals between 5 and 85 °C. The concentrations of the peptide stock solutions were spectrophotometrically estimated.

Gel Mobility Shift Assay. Gel mobility shift assays were basically carried out under the previously described experimental conditions (*21*, *22*). Each reaction mixture contained Tris-HCl (10 mM, pH 8.0), NaCl (50 mM), $ZnCl_2$ (10 μM), dithiothreitol (1 mM), poly(dI-dC) (0 or 25 ng/μL), bovine serum albumin (40 ng/μL), Nonidet P-40 (0.05%), glycerol (5%), the ^{32}P-5′-end-labeled substrate DNA fragment (<50 pM, 500 cpm), and peptide (0−4 μM). After incubation at 20 °C for 30 min, the sample was run on an 8% polyacrylamide gel with TB buffer (89 mM Tris-HCl, and 89 mM boric acid) at 20 °C. The bands were visualized by autoradiography and quantified using ImageMaster 1D Elite software (Ver. 3.01).

High-Sensitivity Isothermal Calorimetry. All experiments were performed in a buffer containing Tris-HCl (10 mM, pH 8.0), NaCl (100 mM), Nonidet P-40 (0.05%) at 25 °C using a VP−ITC MicroCalorimeter (MicroCal, Northampton, USA). The cell volume was 1.426 mL, and the syringe volume was 250 μL. The measurements of the peptide-Zn(II) complex were preformed in the buffer by adding 1.5 equiv of $ZnSO_4$. The peptide (≈25 μM) was titrated in a 10 μL volume per injection into the cell containing the double-stranded DNA solution (≈3 μM). In each experiment, 25 injections were made with a 280 s interval between injections, so that the final molar ratio of the peptide to DNA is 2. The stirring rate was 394 rpm throughout the experiment. All solutions were degassed for 10 min by evacuation. The heat of dilution of the peptide was obtained by titrating peptide into the buffer. The actual heat of the peptide−DNA complex formation was determined after subtracting the heat of dilution of the peptide. The ITC binding curves were analyzed using the single-site binding equation in the MicroCal ORIGIN software package provided by the manufacturer. Each experiment was repeated at least three times using the identical conditions and then the K_d, n, ΔH, and ΔS values were calculated.

RESULTS AND DISCUSSION

Zinc Coordination of GAGA Zinc Finger Mutants. To examine whether the mutants retain the tetrahedral metal coordination geometry like the wild-type peptide, the peptide−metal coordination chemistry was investigated by UV−vis absorption spectroscopy. Zn(II) is a spectroscopically silent ion in the visible region of the electromagnetic spectrum because of the d^{10} electronic configuration. Therefore, the metal coordination of the zinc fingers has often been studied using Co(II) as a spectroscopic probe for the zinc site (*23*, *24*). The UV−vis spectrum of the Co(II) complex of all the mutants is compared to the spectrum of the wild-type peptide (Figure 3A). All mutants display a spectrum similar to the wild-type. The intense absorption bands in the near UV region around 316 and 340 nm are indicative of the $S^- \rightarrow$ Co(II) ligand-to-metal charge transfer (LMCT) transition (*25*). The magnitude of the extinction coefficient (ϵ) at 320 nm reflects the number of thiol-containing ligands coordinated to the metal and averages about 900−1200 M^{-1} cm^{-1} per S^-−Co(II) bond (*26*, *27*). The extinction coefficient (ϵ) values at 320 nm of all the GAGA peptides are around 2000 M^{-1} cm^{-1}, inferring that all the peptides use two thiol groups to bind the metal. Furthermore, it is possible to ascertain the coordination geometry of the Co(II) in the peptide−metal complex based on the ligand-field theory; optical transitions of a tetrahedral Co(II) species exhibit an intense d−d absorption band in the 625 ± 50 nm region due to small ligand-field stabilization energy (*28*). The similar d−d transition at around 650 nm suggests that Co(II) is in a tetrahedral coordination geometry in all the peptides. The titration experiment of these GAGA peptide−Co(II) complex systems clearly showed the 1:1 stoichiometry for the GAGA peptides vs Co(II) (Figure S1, Supporting Information). Competition experiments show that zinc readily displaces cobalt from the complex; the band due to the d−d transition (∼650 nm) observed for the Co(II)-peptide complex disappeared by the addition of an equivalent amount of the spectroscopically silent Zn(II) (Figure 3B). This observation implies that Zn(II) displaces the Co(II) and occupies the tetrahedral site of the peptides due to the ligand-field stabilization energy difference between Co(II) and Zn(II). This result reveals the greater stability of the peptide−Zn(II) complex as shown for the other zinc fingers (*15*, *29*). Thus, the UV−vis data strongly suggest that the mutation in the β-hairpin region does not alter the coordination

[1] Abbreviations: HATU, *O*-(7-azabenzotriazol-1-yl)-1,1,3,3-tetramethyluronium hexafluorophosphate; TMP, 2,4,6-trimethylprodine; RP-HPLC, reverse phase high-performance liquid chromatography; Tris, tris(hydroxymethyl)aminomethane; TB, Tris-boric acid; CD, circular dichroism; ITC, isothermal calorimetry; A.A., amino acid(s).

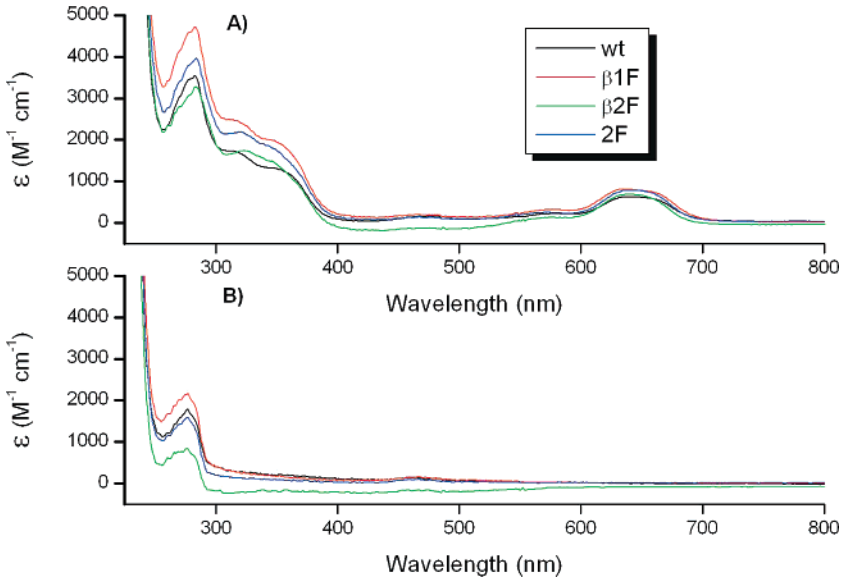

FIGURE 3: UV−vis absorption spectra of (A) Co(II) complexes of GAGA mutant peptides and (B) Co(II) complexes of GAGA mutant peptides in the presence of an equivalent amount of Zn(II).

geometry of the metal binding, i.e., all mutants retain the zinc finger state.

Circular Dichroism Studies. Circular dichroism (CD) spectroscopy is a powerful tool to determine the peptide conformation as well as the DNA structures in solution in a fast and reliable manner (*30*, *31*). Moreover, the CD signature of the zinc finger domain has been well characterized (*13*−*15*, *24*, *32*). Hence, we used CD to obtain the conformational properties of the peptide. The CD spectra of the peptides at 20 °C are shown in Figure 4. All the peptides display a negative band near 200 nm ($\pi \rightarrow \pi^*$ electronic transition) and a shoulder around 222 nm ($n \rightarrow \pi^*$ electronic transition), suggesting that peptides are largely in a random coil conformation with some helical content (≈8%). A significant change in the CD spectrum was observed when $ZnCl_2$ is added; the intensity significantly increases in the helix diagnostic negative molar ellipticity at 222 nm and the random coil signature band near 200 nm with a dramatic reduction in the negative molar ellipticity. These observations indicate that peptides fold into the zinc finger characteristic $\beta\beta\alpha$ fold. As observed for the other fingers, metal ion coordination drives the overall folding of the GAGA zinc finger domain. There is a marginal difference in the helical content between the wild-type peptide and the mutants. The helical content calculated on the basis of the 222 nm band of the wild-type peptide (wt) in the presence of metal is 15%. In the presence of zinc, the helical content of the peptide by phenylalanine substitution in β1 (peptide, β1F) and in β2 (peptide, β2F) were 16 and 13%, respectively. The double substitution (peptide, 2F) slightly decreased the helical content (11%). The marginal differences in the helical content could be due to the minor alteration in the hydrophobic core assembly or the contribution of the aromatic amino acid in the CD spectrum. Although it is difficult to conclude anything with confidence based on the minor differences in the spectra, it is clear that all the peptides display a zinc-finger type CD spectrum in the presence of zinc.

An attempt was made to compare the thermal stability of all the peptides in the presence of Zn(II) by CD. For this purpose, we utilized the zinc finger core alone (30 A.A.)

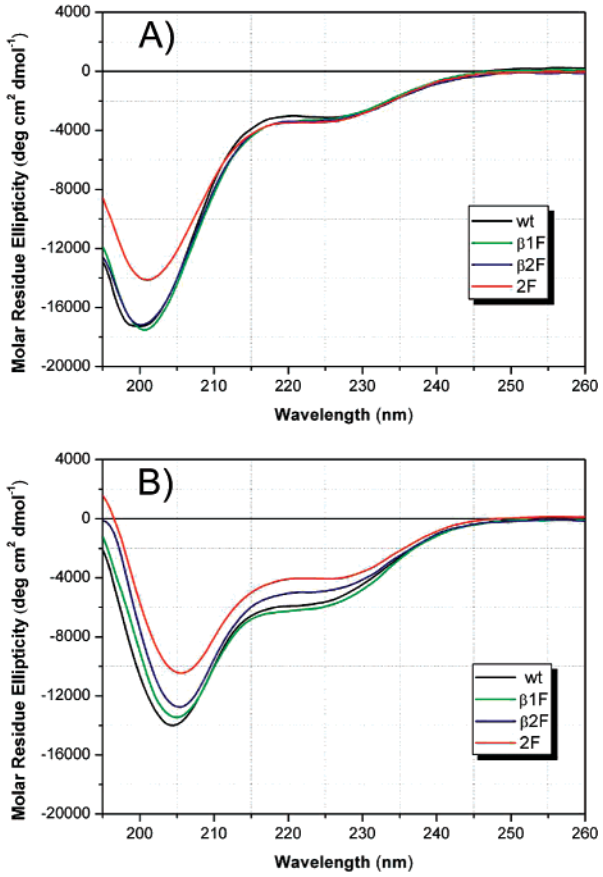

FIGURE 4: Circular dichroism spectra of GAGA mutants (A) in the absence of $ZnCl_2$ and (B) in the presence of $ZnCl_2$ at 20 °C.

without the N-terminal basic region as it was proved that zinc finger core alone is an independent folding unit (*8*, *16*, *23*, *32*). Since the GAGA zinc finger contains mixture of secondary structure, we used $[\theta]_{222nm}$ (helix diagnostic) and $[\theta]_{218nm}$ (β-hairpin diagnostic) to obtain the thermal melting curve. The results are shown in the Figure 5. All the peptides including wild-type exhibited a shallow melting profile, i.e., weakly cooperative folding. Mayo and co-workers showed similar weak cooperative folding for their de novo designed

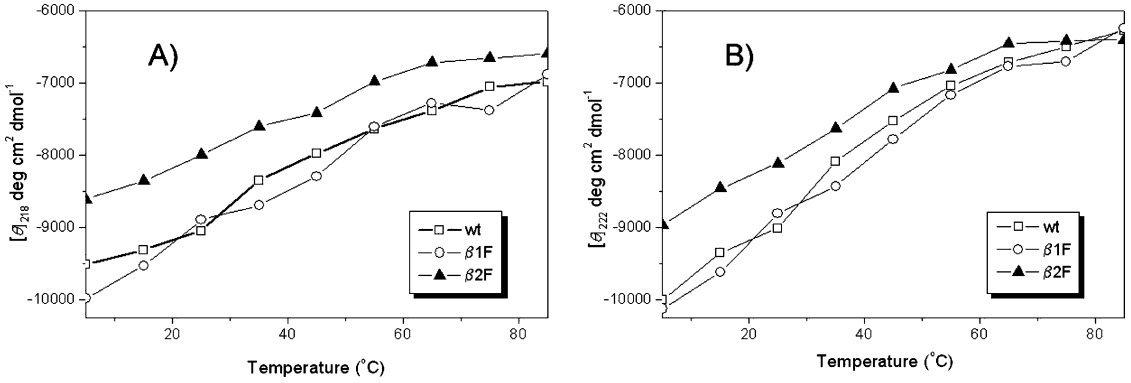

FIGURE 5: Temperature dependence of (A) β-hairpin diagnostic $[\theta]_{218nm}$ and (B) helix diagnostic $[\theta]_{222nm}$.

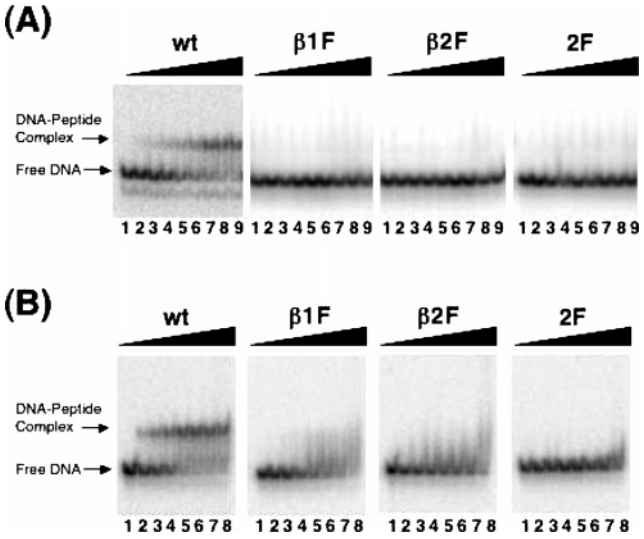

FIGURE 6: Gel mobility shift assays for the peptides binding to the DNA substrates, (A) in the presence of competitor DNA, poly(dI-dC), and (B) in the absence of poly(dI-dC). Lanes 1−9 represent 0, 31, 63, 125, 250, 500, 1000, 2000, and 4000 nM in (A). Lanes 1−8 represent 0, 1, 4, 12, 37, 111, 333, and 1000 nM in (B).

peptide based on zinc finger motif (*14*). The thermal denaturing experiment suggests that the mutation does not affect the thermal stability of the GAGA peptide.

In summary, the CD results suggest that all the peptides folded into zinc finger type fold in the presence of Zn(II).

DNA Binding of GAGA Zinc Finger Mutants. The DNA bindings of the peptides were evaluated by a gel mobility shift assay. These results are shown in Figure 6. Our GAGA wild-type peptide binds to the GAGA specific DNA−substrate in the presence of competitor DNA, poly(dI-dC) (Figure 6A), though smearing bands were observed. In the absence of competitor DNA (Figure 6B), the bound bands were detected at the lower peptide concentration compared with the reaction with competitor DNA. The bound bands of the wild-type peptide were highly smearing. It is indicated that the wild-type peptide nonspecifically interacts with DNA under the condition for the gel mobility shift assay, in which the concentration of the GAGA peptides is much higher (about 20- to 80000-fold) than that of GAGA DNA. The smearing bands may also result from instability of the bound species in the gel. The GAGA mutants, on the contrary, did not present any specific bound bands even in the absence of poly(dI-dC).

Recent studies demonstrated that isothermal calorimetry (ITC) can be successfully used to study specific protein−DNA interactions (*33*). ITC also provides additional information such as the thermodynamics of complex formation, stoichiometry of the complex, and binding constant. This method is relatively simple and also does not need any labeled samples. Most importantly, the protein−DNA interactions can be evaluated in solution by ITC in contrast with gel mobility shift assay. The range of the binding constants directly measured by ITC is between 10^2 and 10^9 M^{-1}, and hence ITC is also suitable to determine the binding constant ($<10^5$ M^{-1}) that is not detected by the gel mobility shift assay. We made an attempt to utilize ITC to check whether the mutant peptides have any weak binding lower than the sensitivity of the gel mobility shift assay. The ITC titration of the peptides into DNA is shown in Figures 7 and 8. An exothermic heat pulse was observed after each injection of the wt peptide into DNA. Each area of this exothermic peak was integrated, and the heat of dilution of the wt peptide was subtracted from the integrated value. The corrected heat was divided by the moles of the injected wt peptide, and the resulting values were plotted as a function of the molar ratio, as shown in Figure 8. The apparent dissociation constant, (K_d), the stoichiometry of binding, (n), the enthalpy change, (ΔH), and the entropy change (ΔS) were measured by fitting the binding isotherms to a single binding site model. The calculated values are as follows: $K_d = 36$ (± 11) nM, $n = 0.997 \pm (0.03)$, $\Delta H = -6.1$ (± 0.3) kcal/mol, and $\Delta S = 13.7$ (± 0.9) cal/mol. The experimental errors were estimated from three independent measurements. Titrations of the zinc complex of the wt peptide into the DNA produced sigmoidal binding curves (Figure 7B) with a stoichiometry of 1.0, indicating that a 1:1 complex is formed. As a control experiment, the wt peptide was titrated against a randomly chosen DNA sequence to differentiate the specific binding from the nonspecific binding. The peaks from the control experiment were indistinguishable from the peaks due to the heats of dilution of the peptide (data not shown), indicating that the wt peptide specifically binds to the cognate DNA and also do not include artifacts due to nonspecific binding.

In the case of the mutant peptides, no specific interactions with DNA could be detected because the titration of mutant peptides with DNA did not yield a sigmoidal curve (Figure 7C,D). The raw calorimetric data of the mutant peptides were very similar to the titration of the peptide into the buffer, buffer into DNA, or peptide into nonspecific DNA substrate. Therefore, both the ITC and gel mobility shift assay confirm that the substitution of an aromatic amino acid in any of the β-strands of β-hairpin abolishes the DNA-binding

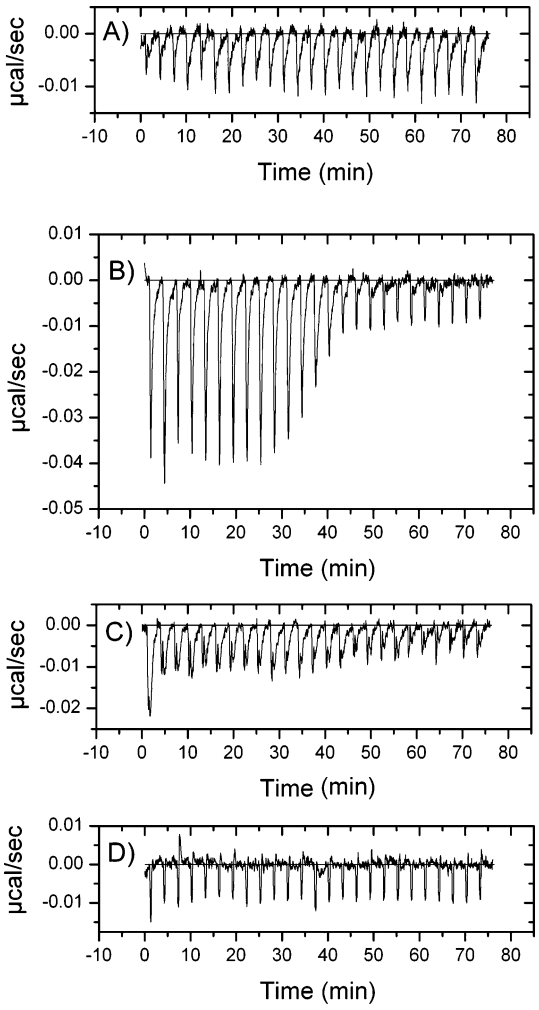

FIGURE 7: Isothermal calorimetric titrations of (A) wt with buffer containing no DNA, (B) wt with DNA, (C) β1F with DNA, and (D) β2F with DNA at 25 °C.

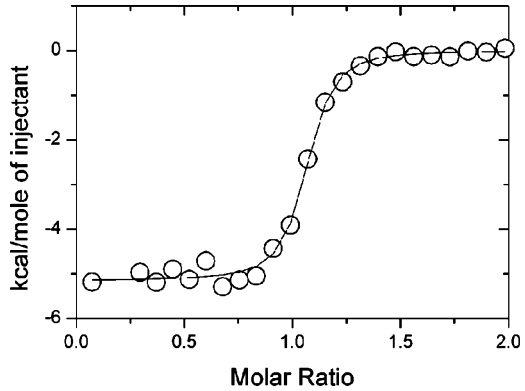

FIGURE 8: Binding isotherm (K_d = 36 ± 11 nM, n = 0.997 ± 0.03, ΔH = −6.1 ± 0.3 kcal/mol and ΔS = 13.7 ± 0.9 cal/mol) obtained from isothermal calorimetric titrations of wild-type peptide with DNA shown in (Figure 7C). The curve has been fit to a 1:1 model to yield the values of n, K_d, ΔH, and ΔS.

ability of the GAGA zinc finger. In addition, our study demonstrated that ITC is useful for evaluating the specific DNA binding of zinc fingers.

The loss of DNA activity of the β2F peptide in which phenylalanine is substituted for isoleucine is plausibly explained by a possible alteration in the minimal hydrophobic core formed by packing of the side-chains from amino acids in the second β-strand (β2) and helix, because the mutant

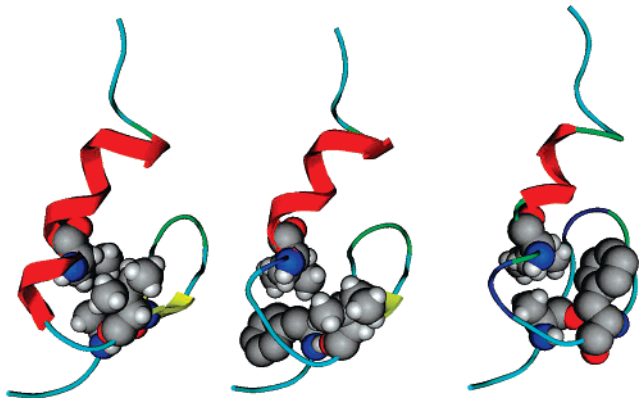

FIGURE 9: Energy-minimized structures of wild-type (left), β-1F (middle), and β-2F(right). The picture was produced on the basis of solution NMR structure of GAGA/DNA complex (PDB code: 1YUJ) using MOE program (Chemical Computing Group, Montreal).

peptide has similar zinc coordination geometry and folding. In general, almost all the structurally characterized zinc fingers prefer hydrophobic amino acids with aromatic side-chain (Phe, Tyr, His) (Figure 1) (*9*, *10*, *34*). It is surprising that GAGA prefers a hydrophobic amino acid with an aliphatic side-chain. The substitution of an aromatic amino acid for the aliphatic amino acid might change the DNA-binding surface of the GAGA peptide as a consequence of the alteration in the hydrophobic packing. The inability of the β2F peptide for a specific DNA binding suggests that the side-chain volume rather than aromaticity is important in keeping the right orientation of the DNA-binding surface, i.e., the helical region to interact with the DNA. We envisaged that substitution of the β-sheet favoring phenylalanine (*35*) in the first β-strand (β1) would provide an additional stability to the zinc finger core rather than the helix favoring the alanine residue. The sequence alignment shows that this position is occupied by a β-sheet favoring aromatic amino acids in almost all other zinc fingers. However, our results evidently demonstrate that this mutant β1F does not bind to the GAGA DNA substrate. Presumably, the β1 of GAGA does not fold into the ideal β-sheet conformation. The DNA-binding specificity in the β1F peptide is probably lost by the local structural perturbation, which leads to the alteration in the DNA-binding surface. These results are in line with our recent observation in which we have shown the importance of β-hairpin by swapping β-hairpin region between Sp1 and GLI zinc finger domains (*18*).

To examine the effect of Phe substitution on the structure, the mutant peptides were subjected to energy minimization calculation using standard protocol available in the MOE program. The PDB structure (PDB code: 1YUJ) from NMR determination was used as a starting structure for the calculations (*9*). The resultant final energy-minimized structures are shown in Figure 9. Substitution of Phe at either of the β-hairpin relaxes the compactness of the minimal hydrophobic core necessary for the compact $\beta\beta\alpha$ fold of the zinc finger domain. Imperiali and co-workers demonstrated that the minimal hydrophobic core is essential for holding together the β-hairpin and α-helix of the zinc finger domain in addition to the metal coordination (*13*). Thus, the loss in DNA binding of the GAGA mutants in our study could be

correlated to the changes in the hydrophobic core which eventually affects the DNA-binding surface.

In conclusion, substitution of the consensus phenylalanine in the β-hairpin region of the minimal DNA-binding domain of GAGA retains the zinc finger state (i.e., the folding and geometry of zinc coordination) but abolishes the specific DNA-binding activity. Although it is difficult to interpret exactly the reason why the mutant peptides showed no DNA-binding activity, it is likely that the mutated GAGA peptides might fold into a conformation slightly different from that of the native GAGA peptide as presented in our experiment. Thus, the loss in the DNA-binding activity could be explained by the alteration in the geometric requirements of the DNA recognition due to the variation in the side-chain packing or in the minimal hydrophobic core (*15*, *17*, *36*). Our experimental evidence supports the role of β-hairpin region in the specific DNA binding (*18*). The present study forms an another example for the existence of the complexity in the interactions of the zinc finger with its cognate DNA sequences and also provides useful information for the structure-based artificial zinc finger design (*37*, *38*).

ACKNOWLEDGMENT

We thank M. Matsumoto (Doshisha University) for CD measurements and energy minimization calculations. We also thank M. Suzuki for her help with UV titration experiments.

SUPPORTING INFORMATION AVAILABLE

Figure S1 shows that the determination of stoichiometry of the Co(II) complexes of GAGA wild-type and mutant peptides. This material is available free of charge via the Internet at http://pubs.acs.org.

REFERENCES

1. Jantz, D., Amann, B. T., Gatto, G. J., Jr., and Berg, J. M. (2004) The design of functional DNA-binding proteins based on zinc finger domains, *Chem. Rev. 104*, 789−799.
2. Durai, S., Mani, M., Kandavelou, K., Wu, J., Porteus, M. H., and Chandrasegaran, S. (2005) Zinc finger nucleases: Custom-designed molecular scissors for genome engineering of plant and mammalian cells, *Nucleic Acids Res. 33*, 5978−5990.
3. Dhanasekaran, M., Negi, S., and Sugiura, Y. (2006) Designer zinc finger proteins: Tools for creating artificial DNA-binding functional proteins, *Acc. Chem. Res. 39*, 45−52.
4. Jamieson, A. C., Miller, J. C., and Pabo, C. O. (2003) Drug discovery with engineered zinc-finger proteins, *Nat. Rev. Drug Discovery 2*, 361−368.
5. Blancafort, P., Segal, D. J., and Barbas, C. F., III (2004) Designing transcription factor architectures for drug discovery, *Mol. Pharmacol. 66*, 1361−1371.
6. Klug, A. (2005) Towards therapeutic applications of engineered zinc finger proteins, *FEBS Lett. 579*, 892−894.
7. Pedone, P. V., Ghirlando, R., Clore, G. M., Gronenborn, A. M., Felsenfeld, G., and Omichinski, J. (1996) The single Cys_2-His_2 zinc finger domain of the GAGA protein flanked by basic residues is sufficient for high-affinity specific DNA binding, *Proc. Natl. Acad. Sci. U.S.A 93*, 2822−2826.
8. Iuchi, S. (2001) Three classes of C_2H_2 zinc finger proteins, *Cell. Mol. Life Sci. 58*, 625−635.
9. Omichinski, J. G., Pedone, P. V., Felsenfeld, G., Gronenborn, A. M., and Clore, G. M. (1997) The solution structure of a specific GAGA factor-DNA complex reveals a modular binding mode, *Nat. Struct. Biol. 4*, 122−132.
10. Padmanabhan, S., Marqusee, S., Ridgeway, T., Laue, T. M., and Baldwin, R. L. (1990) Relative helix-forming tendencies of nonpolar amino acids, *Nature 344*, 268−270.
11. O'Neil, K. T., and DeGrado, W. (1990) A thermodynamic scale for the helix-forming tendencies of the commonly occurring amino acids, *Science 250*, 646−651.
12. Berg, J., and Godwin, H. A. (1997) Lessons from zinc-binding peptides, *Annu. Rev. Biophys. Biomol. Struct. 26*, 357−371.
13. Struthers, M. D., Cheng, R. P., and Imperiali, B. (1996) Design of a monomeric 23-residue polypeptide with defined tertiary structure, *Science 271*, 342−345.
14. Dahiyat, B. I., and Mayo, S. T. (1997) De novo protein design; Fully automated sequence selection, *Science 278*, 82−87.
15. Weiss, M. A., and Keutmann, H. (1990) Alternating zinc finger motifs in the male-associated protein ZFY: Defining architectural rules by mutagenesis and design of an "aromatic swap" second-site revertant, *Biochemistry 29*, 9808−9813.
16. Lachenmann, M. J., Ladbury, J. E., Philips, N. B., Narayana, N., Qian, X., and Weiss, M. A. (2002) The hidden thermodynamics of a zinc finger, *J. Mol. Biol. 316*, 969−989.
17. Mortishire-Smith, R. J., Lee, M. S., Bolinger, L., and Wright, P. E., (1992) Structural determinants of Cys_2His_2 zinc fingers, *FEBS Lett. 296*, 11−15.
18. Shiraishi, Y., Imanishi, M., Morisaki, T., and Sugiura, Y. (2005) Swapping of the β-hairpin region between Sp1 and GLI zinc fingers: Significant role of the β-hairpin region in DNA binding properties of C_2H_2-type zinc finger peptides, *Biochemistry 44*, 2523−2528.
19. Negi, S., Dhanasekaran, M., Urata, H., and Sugiura, Y. (2006) Biomolecular mirror-image recognition: Reciprocal chiral-specific DNA binding of synthetic enantiomers of zinc finger domain from GAGA factor, *Chirality 18*, 254−258.
20. Nokihara, K., Nagawa, Y., Hong, S.-P., and Nakanishi, H. (1997) Efficient solid-phase synthesis of a large peptide by a single coupling protocol with a single HPLC purification step, *Lett. Pept. Sci. 4*, 141−146.
21. Uno, Y., Matsushita, K., Nagaoka, M., and Sugiura, Y. (2001) Finger-positional change in three zinc finger protein Sp1: influence of terminal finger in DNA recognition, *Biochemistry 40*, 1787−1795.
22. Shiraishi, Y., Imanishi, M., and Sugiura, Y. (2004) Exchange of histidine spacing between Sp1 and GlI zinc fingers: distinct effect of histidine spacing-linker region on DNA binding, *Biochemistry 43*, 6352−6359.
23. Frankel, A. D., Berg, J. M., and Pabo, C. O. (1987) Metal-dependent folding of a single zinc finger from transcriptional IIIA, *Proc. Natl. Acad. Sci. U.S.A. 84*, 4841−4845.
24. Nomura, A., and Sugiura, Y. (2002) Contribution of individual zinc ligands to metal binding and peptide folding of zinc finger peptides, *Inorg. Chem. 41*, 3693−3698.
25. Giedroc, D. P., Keating, K. M., Williams, K. R., Konigsberg, W. H., Coleman, J. E. (1986) Gene 32 protein, the single-stranded DNA binding protein from bacteriophage T4, is a zinc metalloprotein, *Proc. Natl. Acad. Sci. U.S.A. 83*, 8452−8456.
26. May, S. W., and Kuo, J.-Y. (1978) Preparation and properties of cobalt(II) rubredoxin, *Biochemistry 17*, 3333−3338.
27. Vašák, M., Kägi, J. H. R., Holmquist, B., Vallee, B. L.(1981) Spectral studies of cobalt(II)- and nickel(II)-metallothionein, *Biochemistry 20*, 6659−6664.
28. Bertini, I., and Luchinat, C. (1984) High spin cobalt(II) as a probe for the investigation of metalloproteins, *Adv. Inorg. Biochem. 6*, 71−111.
29. Berg, J. M., and Merkle, D. L. (1989) On the metal ion specificity of "zinc finger" proteins, *J. Am. Chem. Soc. 111*, 3759−3761.
30. Woody, R. W. (1995) Circular dichroism, *Methods Enzymol. 246*, 34−71.
31. Gray, D. M., Ratliff, R. L., and Vaughan, M. R. (1992) Circular dichroism spectroscopy of DNA, *Methods Enzymol. 211*, 389−406.
32. Parraga, G., Horvath, S. J., Eisen, A., Taylor, W. E., Hood, L., Young, E. T., and Klevit, R. E. (1988) Zinc-dependent structure of a single-finger domain of yeast ADR1, *Science 241*, 1489−1492.
33. Elrod-Erickson, M., Rould, M. A., Nekludova, L., and Pabo, C. O. (1996) Zif268 protein-DNA complex refined at 1.6 Å: A model system for understanding zinc finger-DNA interactions. *Structure 4*, 1171−1180.
34. Michael, S. F., Kilfoil, V. J., Schmidt, M. H., Amann, B. T., and Berg, J. (1992) Metal binding and folding properties of a minimalist Cys_2His_2 zinc finger peptide, *Proc. Natl. Acad. Sci. U.S.A. 89*, 4796−4800.

35. Kim, C. A., and Berg, J. M. (1993) Thermodynamic β-sheet propensities measured using a zinc-finger host peptide, *Nature 362*, 267−270.
36. Kochoyan, M., Keutmann, H. T., and Weiss, M. A. (1991) Architectural rules of the zinc-finger motif: Comparative two-dimentional NMR studies of native and "aromatic-swap" domains define a "weakly polar switch", *Proc. Natl. Acad. Sci. U.S.A 88*, 8455−8459.
37. Wolfe, S. A., Grant, R. A., Elrod-Erickson, M., and Pabo, C. O. (2001) Beyond the "recognition code"; Structures of two Cys_2-His_2 zinc finger/TATA box complexes, *Structure 9*, 717−723.
38. Miller, J. C., and Pabo, C. O. (2001) Rearrangement of side-chains in a Zif268 mutant highlights the complexities of zinc finger-DNA recognition, *J. Mol. Biol. 313*, 309−315.

BI700009Q